SYSTEMS AND COMPUTER ENGINEERING

OFDMA Return-link for Multimedia Interactive Terrestrial Broadcasting System: Diversity Techniques for Mobile and Portable Terminals

Carleton
UNIVERSITY

Department of Systems and Computer Engineering
Car leton University, 1125 Colonel By Drive
Ottawa, Ontario, Canada K1S 5B6

OFDMA Return-link for Multimedia Interactive Terrestrial Broadcasting System: Diversity Techniques for Mobile and Portable Terminals

Prepared By

Mohamed S. El-Tanany, Ph.D., P.Eng

Department of Systems and Computer Engineering
Carleton University,1125 Colonel By Drive
Ottawa, Ontario, K1S 5B6

Prepared for

Communications Research Centre
3701 Carling Avenue,Shirley Bay, Ottawa, Ontario

Contract Number: U6800-0-0510
Scientific Authority: Dr. Yiyan Wu

March, 2002

OFDMA Return-link for Multimedia Interactive Terrestrial Broadcasting System: Diversity Techniques for Mobile and Portable Terminals

1. Introduction

This document discusses the performance of OFDM when used as a modulation and access technique for the return-link of an interactive broadcast system. In such an application, the return-link performance becomes strongly dependent on the temporal variations of the channels presented to individual uplink users. The uplink performance is also heavily affected by equipment imperfections which result-in uncorrelated frequency and sampling clock errors for different users uplink signals.

In a previous study, the impact of equipment imperfections, on the uplink performance, has been quantified both analytically and by computer simulation. The study assumed no diversity reception. The results of the previous study suggested that OFDMA presented a viable option for the return-link multiplexing. The SNR requirements for raw error rates in the range 10^{-3} were found to be rather high.

This report investigates a number of return-link modulation techniques and quantifies their performance, assuming second order diversity (either frequency diversity or antenna diversity). Throughout this study uplink users are assumed to be presented with non-correlated flat fading channels with the Doppler spread as a parameter. The modulation techniques considered are those that have been proven to work in single-carrier systems over fading channels.

The main finding of this study is that diversity techniques, such as head-end receiving antenna diversity and more effectively return-link carrier diversity, can significantly improve the receiving conditions in a flat Rayleigh fading channel for mobile or portable receptions. The study shows that, with diversity, more than 10 dB S/N gain can be achieved for $\pi/4$- DQPSK, $\pi/8$-D8PSK or 16QAM modulated multiple access OFDM systems. Diversity also improves the robustness against Doppler effect, carrier and sampling frequency errors. Multiple access OFDM is robust to the return-link transmitter time-synchronization. As long as the synchronization error is within the OFDM guard interval. The return-link timing errors can be corrected by a one-tap equalizer at the head-end.

1.1 Access Technique

The advantages of using OFDM as a return-link access technique, some times referred to as OFDMA, are:

1. *Spectrum efficiency*: Return-link carriers, or OFDM carriers, can overlap, which eliminates the need of guard band used in the FDMA approach.

2. *Flexibility*: One or multiple OFDM carriers can be assigned to each return-link user, depending on the service/traffic requirements. Modulation technique of different orders (QPSK, 16QAM, 64QAM, etc.) can be used on different OFDM carriers, depending on the quality of the return link channel between the hub receiver and the specific location of the user terminal. This reflects on the return-channel capacity.
3. *Robustness* to multipath distortion: a guard interval can be inserted between each transmitted symbol to mitigate multipath distortion. Each return-link user terminal should insert a guard interval to reduce intersymbol interference. By lengthening the period of the symbols transmitted on each OFDM carrier, the actual bandwidth of these carriers becomes relatively small and the fading caused by channel multipath can be assumed to produce flat fading on these carriers resulting in Rayleigh fading. The reliability of the return channel augments with its capacity, i.e., higher the capacity is, larger is the number of carriers used and, if proper frequency interleaving is used, smaller is the probability that all the needed carriers will be faded. At one extreme, a return channel with only one carrier will experience Rayleigh fading which can be randomized through frequency hopping or diversified reception at the headend. At the other extreme, if the whole channel is used by one return channel user, frequency interleaving will allow for the same robustness as experienced on a broadcast link using a full complement of OFDM carriers.

A previous study provided the analytical tools necessary to quantify the performance of such a return-link by taking into account the presence of non-correlated carriers, clock, and timing errors of all return-link users. The present report deals with the uplink performance subject to non-correlated Rayleigh fading, with and without diversity reception..

1.2 Transmission Technique

OFDM provides an effective method to mitigate the intersymbol interference (ISI) when wideband signaling over multipath radio channels is used. The main idea is to send the data in parallel over a number of narrow-band flat fading subchannels. This is efficiently achieved by using a set of overlapping orthogonal signals to partition the channel. The transceiver can be realized using a number of coherent QAM modems which are equally spaced in the frequency domain, and which can be implemented by using the IDFT at the transmitter and the DFT at the receiver. However, due to the fact that the intercarrier spacing in OFDM is relatively small, OFDM transceivers are somewhat more sensitive to phase noise, frequency errors and sampling clock frequency errors by comparison to single carrier transceivers.

For an interactive broadcasting, OFDM clearly offers the advantage of ISI avoidance over frequency selective channels when used on the downlink. Its performance on the return-link remains unclear since only a few of the OFDM carriers would be used per each user terminal depending on the channel capacity required. The frequency redundancy would be reduced by this fact. Previous work dealt with the sensitivity of OFDM to phase noise, frequency errors and sampling clock frequency errors. The purpose of this document is to quantify the return link performance when subjected to non-correlated Rayleigh fading.

The advantages of using OFDM as a return-link transmission technique are:

- ISI avoidance on the return-link; this becomes more apparent as the transmission bandwidth increases.

- Provides a high level of flexibility in terms of frequency resource allocation; for example, a user may be assigned one OFDM carrier, or a "tone" for a certain period of time or, depending on his/her traffic requirements, several OFDM carriers simultaneously.
- From an end user equipment perspective, it is preferable to give individual users as few OFDM carriers as possible at any given time. The motivation here is to maintain the signal peak-to-average power ratio as low as possible while increasing the transmission range (distance).
- In the event an individual user is assigned several OFDM carriers, they must be spaced sufficiently far apart in order to exploit the frequency diversity of the channel.

In our investigation, it is assumed that each OFDM carrier during an OFDM return-link symbol is assigned to a different user. As a result, as seen by the base station, each OFDM carrier will experience a different channel, carrier frequency error, sampling frequency error and a different delay. Our investigation considers uncoded OFDM with the understanding that a raw error rate of 10^{-2} to 10^{-3} represents an acceptable performance threshold since FEC is likely to improve it by several orders of magnitude.

In such a case, ISI is assumed to be eliminated but each return link will suffer from the outage created by a Rayleigh flat fading channel. The performance of the return link will be quantified according to this Rayleigh flat fading. Antenna diversity techniques can be implemented at the head-end, which can significantly improve the system performance over the fading channel. Flexible carrier assignment and carrier hopping can also be used to implement uplink frequency diversity.

1.3 System Model

The model used for simulating the return-link performance is shown in Figure 1. The main features of this model are the following:

- Each return-link user transmits only one information symbol per OFDM symbol. The information symbol is represented as a complex constellation point and denoted by a_l in Figure 1. The exact nature of the constellation point depends on the base-band modulation method used. In this document we consider $\pi/4$-DQPSK, $\pi/8$-D8PSK and 16QAM.
- The information symbol is applied to a single-side-band (SSB)[1] modulator with a nominal carrier frequency f_0. The modulator output for a given user will be a single frequency sinusoid of duration equal to an OFDM symbol period plus a guard interval.
- The nominal frequency of the lth SSB modulator is $f_0 + l/T^{-1}_{\text{OFDM}} + \delta_{cf}$, where T_{ofdm} is the OFDM symbol period as seen by the lth user and which is affected by the sampling clock
- errors. The term δ_{cf} is the carrier frequency error caused by the lth user equipment (Doppler shift is accounted for in the channel model).

---

1. SSB modulators and demodulators have been used in this study, as they are more tractable for analysis and simulation purposes. The results presented also apply to the case in which quadrature modulators/demodulators are used. The only difference is that the sampling clock errors will be reduced since the sampling clock frequency is reduced by a factor of 2.

- The carrier frequency errors of all users for a given OFDM symbol are generated using a random number generator with a uniform distribution.
- A separate uniform random number generator provides the sampling clock errors, for all return-link users.
- The sets of carrier frequency and sampling clock frequency errors applied to the return-link are changed from one OFDM symbol to the next.
- The SSB modulators' outputs are applied to separate channels. The channel responses are jointly complex Gaussian and are generated using Rayleigh fading simulators (one for each subchannel).
- The front-end of the base station's receiver is modeled as a summing junction for all return-link users. Thermal noise is then added to the combined signal.
- The combined signal plus noise is applied to a down converter with a nominal carrier frequency f_0 and then it is applied to an FFT demodulator.
- The desired component of each FFT coefficient represents an information symbol scaled in magnitude by the channel. It is also rotated in phase due to the channel, random carrier and sampling frequency errors and also due to random delays.
- The FFT output is applied to a differentially coherent detector, in the case of π/4-DQPSK and π/8-D8PSK. In the case of 16QAM, the FFT output is applied to a frequency-domain equalizer, followed by a slicer.
- For diversity reception, we implemented maximal ratio post-detection combining for 16QAM. Equal gain post-detection combining is used for π/4-DQPSK and π/8-D8PSK.

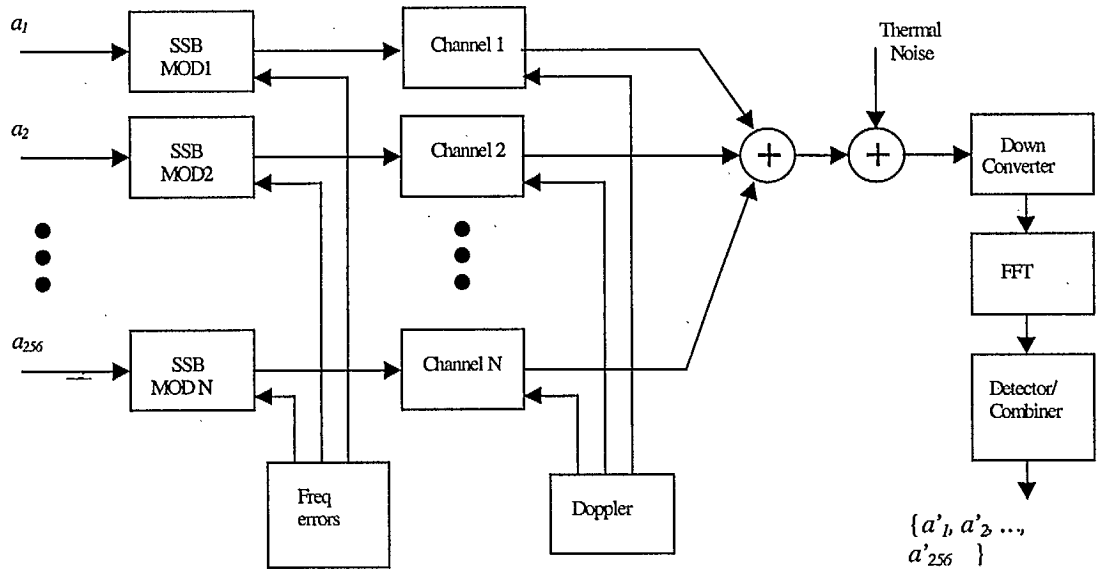

Figure 1Uplink Simulation Model

2. Base-band Modulation Techniques

We considered the following three modulation techniques, which are suitable for Rayleigh fading channels.

2.1) π/4-DQPSK SIGNAL MAPPING

In this case the transmitter encodes data symbols[2] into the phase changes of the modulated carrier. The differential carrier phase, $\Delta\theta(n)$ during the interval (n-1)T[3] and nT is related to the absolute carrier phase, $\theta(n)$ as follows :

$$\Delta\theta(n) = \theta(n) - \theta(n-1) \qquad (1)$$

The mapping from data symbols (a_n b_n) to phase differences ($\Delta\theta(n)$) is rather arbitrary. However, it is preferable to use gray coding. This will ensure that, most of the time, one symbol error causes one bit error. The mapping used in this study is shown in table I.

Table I: Differential phase assignments for π/4DQPSK

a_n b_n	$\Delta\theta$
1 1	-3π/4
1 0	-π/4
0 0	π/4
0 1	3π/4

The carrier-phase during the nth OFDM symbol interval is given by:

$$\theta(n) = \sum_{l=0}^{n} \Delta\theta(l) \qquad (2)$$

Where $\Delta\theta(l)$ assumes the values shown in table I. Based on equation (2) it can be concluded that the absolute phase $\theta(n)$ takes on the values $\{\pm\pi/4, \pm 3\pi/4\}$ for n odd , and $\{0, \pm\pi/2, \pi\}$ for n even. As a result, the signal constellation[4] has 8-states as shown in figure 2.

---

[2] One symbol consists of two consecutive bits
[3] T is the OFDM symbol period

Differentially Coherent demodulation of π/4-DQPSK

The data detection may be accomplished using a differentially coherent demodulator. The differentially coherent approach uses a noisy phase reference (the received signal over the previous symbol period) instead of a recovered carrier; hence a loss in performance compared to a fully coherent demodulator. The differential detector measures phase changes over one symbol period and compares the measured phase difference to the assignments given in table I. The differential detector has two main advantages in our application:

a) Channel estimation for uplink carriers is not needed

b) It has a relatively low implementation loss by comparison to fully coherent detectors.

Its performance in can be improved (for slowly varying channels) by using multiple symbol delays, followed by a sequence estimator.

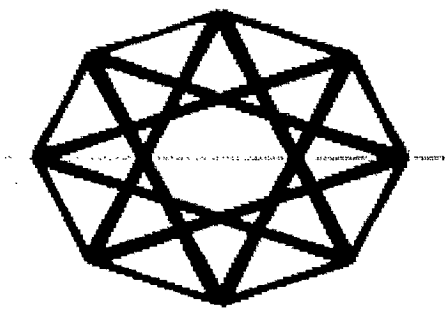

Figure 2 Constellation diagram of π/4 DQPSK

2.2) π/8-D8PSK SIGNAL MAPPING

In this case the transmitter encodes data symbols[5] into the phase changes of the modulated carrier. The differential carrier phase, $\Delta\theta(n)$ during the interval (n-1)T[6] and nT is related to the absolute carrier phase, $\theta(n)$ as follows :

$$\Delta\theta(n) = \theta(n) - \theta(n-1) \qquad (3)$$

---

[4] a complex-plane plot of the signal's complex envelope $\exp[j\theta(n)]$

[5] One symbol consists of three consecutive bits

[6] T is the OFDM symbol period

The mapping from data symbols ($a_n\ b_n\ c_n$) to phase differences ($\Delta\theta(n)$) is rather arbitrary. However, it is preferable to use gray coding. This will ensure that, most of the time, one symbol error causes one bit error. The mapping used in this study is shown in table II.

Table II: Differential phase assignments for π/8 D8PSK

$a_n\ b_n\ c_n$	$\Delta\theta$
1 1 1	$7\pi/4$
0 1 1	$5\pi/4$
0 0 1	$3\pi/4$
0 0 0	$\pi/4$
0 1 0	$-\pi/4$
1 1 0	$-3\pi/4$
1 0 0	$-5\pi/4$
1 0 1	$-7\pi/4$

The carrier phase during the nth OFDM symbol interval is given by:

$$\theta(n) = \sum_{l=0}^{n} \Delta\theta(l) \qquad (4)$$

Where $\Delta\theta(l)$ assumes the values shown in table II. Based on equation (4) it can be concluded that the absolute phase, $\theta(n)$ takes on the values $\{\pm\pi/8, \pm3\pi/8, \pm5\pi/8, \pm7\pi/8\}$ for n odd, and $\{0, \pm\pi/4, \pi, \pm\pi/2, \pm3\pi/4\}$ for n even. As a result, the signal constellation[7] has 16-states as shown in figure 3.

[7] a complex-plane plot of the signal's complex envelope $\exp[j\theta(n)]$

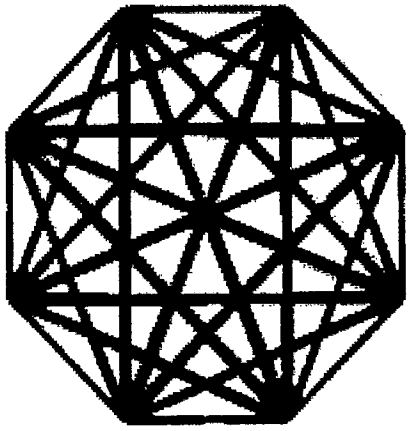

Figure 3 Constellation diagram of π/8 D8PSK

Differentially Coherent demodulation of π/8-D8PSK

The data detection may be accomplished using a differentially coherent demodulator. The differentially coherent approach uses a noisy phase reference (the received signal over the previous symbol period) instead of a recovered carrier; hence a loss in performance compared to a fully coherent demodulator. The differential detector measures phase changes over one symbol period and compares the measured phase difference to the assignments given in table II. The differential detector has two main advantages in our application:

c) Channel estimation for uplink carriers is not needed

d) It has a relatively low implementation loss by comparison to fully coherent detectors.

Its performance can be improved (for slowly varying channels) by using multiple symbol delays, followed by a sequence estimator.

2.3) **16QAM, pilot-assisted**

16QAM is spectrally efficient as it allows the transmission of 4 bits per information symbol. Here the information affects both the amplitude and phase of the transmitted carrier. As a result, it is not possible to use differentially coherent demodulation as was the case with DPSK. 16QAM demodulation requires the knowledge of the carrier phase and amplitude for each symbol. Several methods [2] have been proposed to provide the amplitude and phase information

required for coherent demodulation. One method [3] that has been claimed to be effective for fast fading requires the periodic transmission of pilot symbols. For data rates of 64 kb/s, the pilot symbol is transmitted every 16 symbol intervals to ensure proper operation in fast fading.

3. Symbol Error Rate performance

The average probability of error for the three modulation techniques, when used in single-carrier systems, has been reported in the open literature.

$\pi/4$ DQPSK BER performance in Rayleigh fading is given in [4]

$$P = \frac{1}{2}\left(1 - \frac{\overline{E_B}/N_0}{\sqrt{1/2 + 2\overline{E_B}/N_0 + (\overline{E_B}/N_0)^2}}\right) \tag{5}$$

where $\overline{E_B} / N_0$ is the average energy-per-bit to noise density ratio

For DMPSK the SER for Rayleigh flat fading (no diversity) is given in [5] by

$$\overline{P} = \frac{1}{\pi}\int_0^{\pi(1-1/M)} \frac{1}{1+\overline{z}B(\phi)}d\phi \tag{6}$$

where

$$z = \overline{E_s} / N_0$$

and

$$B(\phi) = \frac{\sin^2(\pi/M)}{1+\cos(\pi/M)\cos\phi}$$

The SER for DMPSK over Rayleigh fading channels in the presence of L-order receiver diversity is given in [5] by:

$$\overline{P} = \frac{1}{\pi}\int_0^{\pi(1-1/M)} \frac{1}{[1+\overline{z}B(\phi)]^L}d\phi \tag{7}$$

where

$$z = \overline{E_s} / N_0$$

and

$$B(\phi) = \frac{\sin^2(\pi/M)}{1+\cos(\pi/M)\cos\phi}$$

The SER performance for 16QAM in flat Rayleigh fading (no diversity) is given in [1] by:

$$\overline{P_e} = 2\cdot\left(1-\frac{1}{\sqrt{M}}\right)\cdot(1-\xi) - \left(1-\frac{1}{\sqrt{M}}\right)^2\cdot\left[1-2\cdot\xi+\frac{4}{\pi}\cdot\xi\cdot a\tan(\xi)\right] \quad (8)$$

where

$$\xi = \sqrt{\frac{a}{1+a}}$$

and

$$a = \frac{3\bar{\gamma}}{2(M-1)}$$

4. Simulation Parameters

Number of sub-carriers	256 (sub-carriers 1 and 129 carry no data)
FFT size	512
Channel Model	Flat Rayleigh fading (Jakes model). Different channel for each sub-carrier
Maximum Doppler	In a range from .5% to 2% relative to subcarrier spacing
Carrier frequency errors	Uniformly distributed, statistically independent
Sampling clock errors	Uniformly distributed, statistically independent
Modulation Methods	π/4-DQPSK, π/8-D8PSK or 16QAM;
Channel estimates	assumed ideal in the case of 16QAM. Not needed for π/4-DQPSK, π/8-D8PSK
Diversity Combining	Maximal Ratio, post-detection (i.e. at output of FFT) for 16QAM. Equal gain, post-detection (i.e. at output of differential detector) for π/4-DQPSK and π/8-D8PSK
No. of OFDM symbols	2048

5. Simulation Results

Figure 4 shows the SER performance curves based on the analytical expressions presented by equations 5-8. These results clearly indicate that:

In the absence of diversity, the SER performance of D8PSK and coherent 16QAM are almost identical. It should be noted that D8PSK has a lower spectral efficiency (<3 bits per Hz) compared to 16QAM which has a spectral efficiency bound of 4 bits per Hz. It should also be noted that D8PSK is much simpler to implement and requires no training overhead. 16QAM requires some kind of channel tracking based on repeated transmissions of pilot symbols.

With second order diversity, the SER performance for D8PSK is significantly improved. The diversity gain measured at SER of 10^{-3} is nearly 15 dB.

The SER performance for DQPSK is clearly superior to D8PSK in the absence and in the presence of diversity, as would be expected.

Figure 5 shows the simulation results obtained for $\pi/4$ DQPSK with and without diversity, with the channel Doppler spread as a parameter. Figure 5 reveals that:

The simulation results for no diversity are within 0.5 dB of the analytical results (figure 4)

The simulation results, with diversity, for a Doppler spread of 0.5% (relative to the sub-carrier spacing) are also within 0.5 dB compared to the analytical results for second order diversity reception.

The Doppler spread has a significant impact on the SER for error rates below about 10^{-4}. The impact is less pronounced for error rates around 10^{-3}.

Increasing the Doppler spread form 0.5% to 2% causes a reduction in diversity gain of about 2 dB at an error rate of 10^{-3}.

Figure 6 shows the simulation results for $\pi/4$ DQPSK converted into BER vs. E_b/N_0.

Figure 7 shows the simulation results obtained for $\pi/8$ D8PSK, with no diversity and also with second order diversity. The results are presented for a range of Doppler spreads. These results clearly indicate that:

The static, no diversity results closely match the analytical performance curve shown in figure 4. The no-diversity performance curves deteriorate quite rapidly with the increase of Doppler spread.

The second order diversity results with a Doppler of 0.5% (in addition to non-correlated frequency errors of 0.5%) are within 1 dB by comparison to the analytical, ideal second order diversity results.

Increasing the both Doppler spread and the carrier frequency errors form 0.5% to 1%, causes a reduction in diversity gain by about 2 dB.

Continued increase in Doppler spread eventually leads to an irreducible error floor. This is to be expected as a result of increase in the frequency of deep-fades which are accompanied by channel-caused phase hits (which can not be rectified by a differentially coherent receiver).

Figure 8 shows the simulation results for D8PSK but converted into BER versus Eb/N0.

Figure 9 shows the simulation results obtained for 16QAM, with no diversity and also with second order diversity. The results are presented for a range of Doppler spreads. These results clearly indicate that:

In absence of diversity the simulation results closely match the analytical results of figure 4.

For a Doppler spread of 1%, in addition to non-correlated frequency errors of 1%, the 16QAM performance is close to that of D8PSK under static conditions.

The 16QAM results seem less sensitive to Doppler spread compared to D8PSK. This observation should however be interpreted in light of the fact that the 16QAM results are based on a perfect knowledge of all uplink channels. In a realistic scenario, the channels will be estimated based on pilot symbols. Practical channel estimates are likely to cause a loss in performance by more than 1 dB as noted in [3].

Figure 10 shows the 16QAM results as BER vs. Eb/N0.

6. Conclusions

Based on the results presented, without diversity, all three modulation schemes require unrealistic S/N under flat Rayleigh fading conditions. For SER = 2.0×10^{-3}, the required S/N > 30 dB. Excessive transmission power is needed to support the required S/N level and frequency errors and phase noise can further degrade the system performance. Using diversity, for SER = 2.0E-3, more than 10 dB diversity gain can be achieved for various Doppler shifts (f_d), sampling frequency errors (Δf) and carrier frequency errors (Δf). With Doppler effects (f_d = 1% relative to the sub-carrier spacing), carrier and sampling frequency errors ($\Delta f_{carrier}$ = 1% and $\Delta f_{sampling}$= 10PPM), the S/N degradation is only less than 1 dB for all modulation schemes. At lower SER, the diversity gains are much higher.

Multiple access OFDM is robust to the return-link transmitter synchronization. As long as the synchronization error is within the OFDM guard interval. The return-link timing errors can be corrected by a one-tap equalizer at the head-end.

We conclude that multiple access OFDM is a good candidate for the Terrestrial Wireless Interactive Multi-media service return link implementation, as described in the DVB-RCT. Diversity techniques, such as head-end receiving antenna diversity and more effectively return-

link carrier diversity, can significantly improve the receiving conditions in a flat Rayleigh fading channel for mobile or portable receptions.

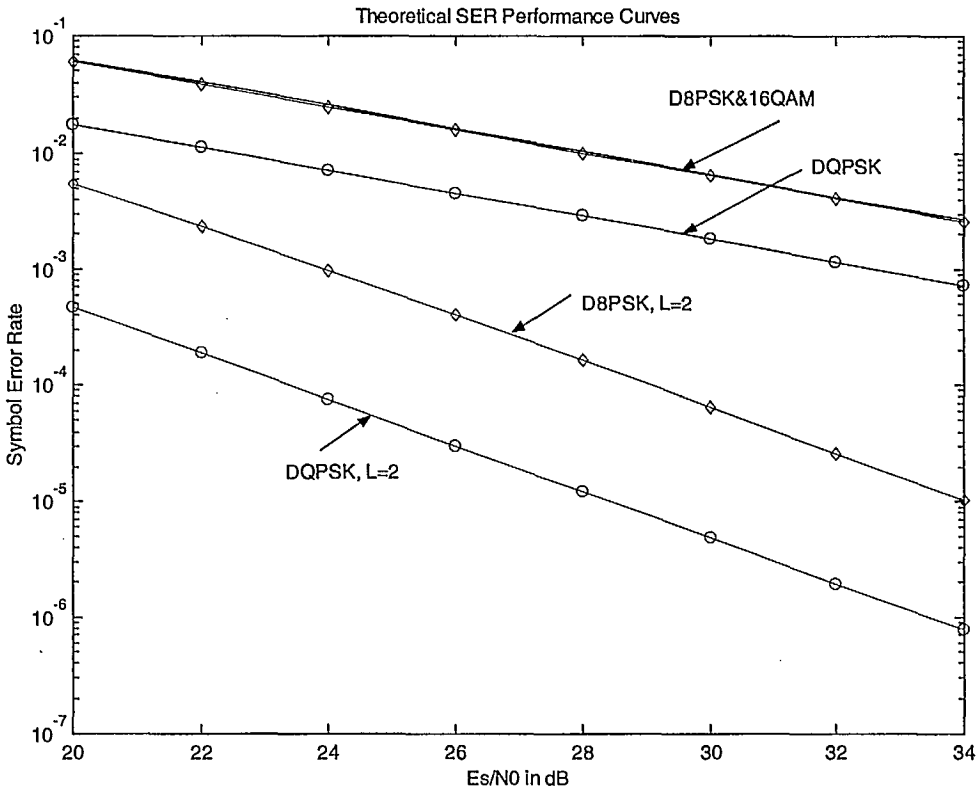

Figure 4 Theoretical SER performance curves for Rayleigh flat fading channels, with and without diversity. It should be noted that the performance of 16QAM (coherent) and that for D8PSK, with no diversity, are very similar. The diversity curves are based on second order receiver diversity. The receiver uses Maximal Ratio combining.

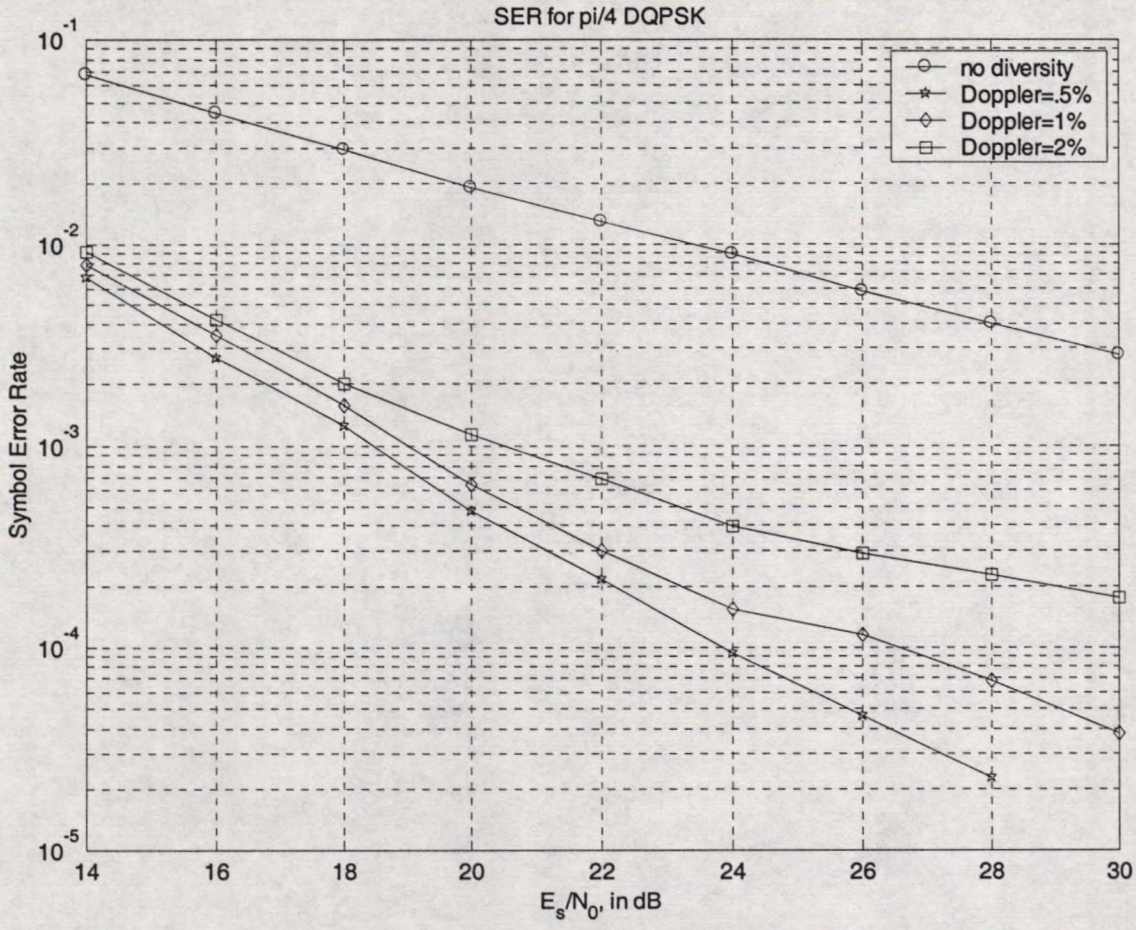

Figure 5 Symbol Error rate for p/4 DQPSK. The maximum Doppler for, the diversity curves, is indicated in the legend as a percentage of the sub-carrier spacing. The up-link carrier frequency errors are uniformly distributed over a range of –1% to +1% relative to the sub-carrier spacing.

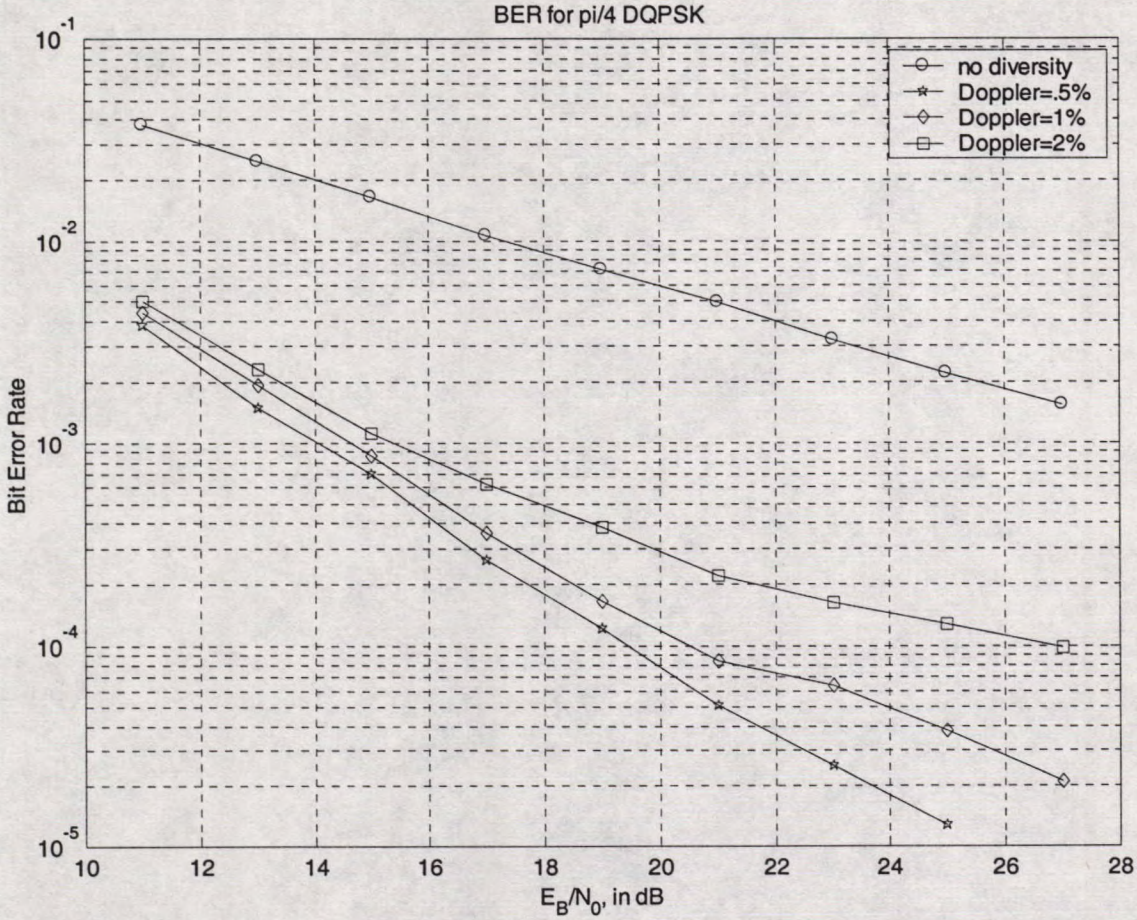

Figure 6 Bit Error rate for π/4 DQPSK. The maximum Doppler for, the diversity curves, is indicated in the legend as a percentage of the sub-carrier spacing. The up-link carrier frequency errors are uniformly distributed over a range of –1% to +1% relative to the sub-carrier spacing. The sampling clock errors are uniformly distributed in a range –10 to +10 PPM.

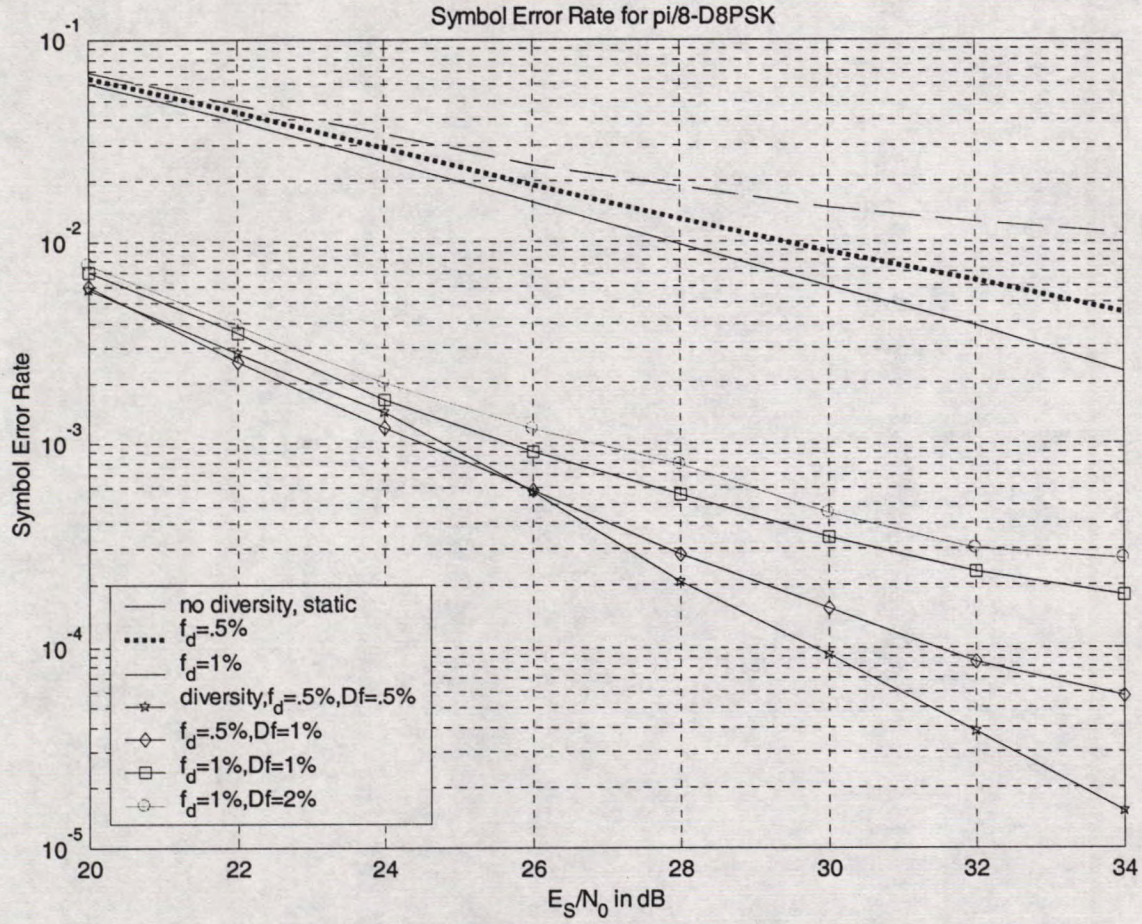

Figure 7 Symbol Error rate for π/8 D8PSK. The maximum Doppler (f_d) is indicated in the legend as a percentage of the sub-carrier spacing. The up-link carrier frequency errors are uniformly distributed over a range of $-\Delta f$ to $+\Delta f$ as shown in the legend. The sampling clock errors are uniformly distributed in a range –10 to +10 PPM.

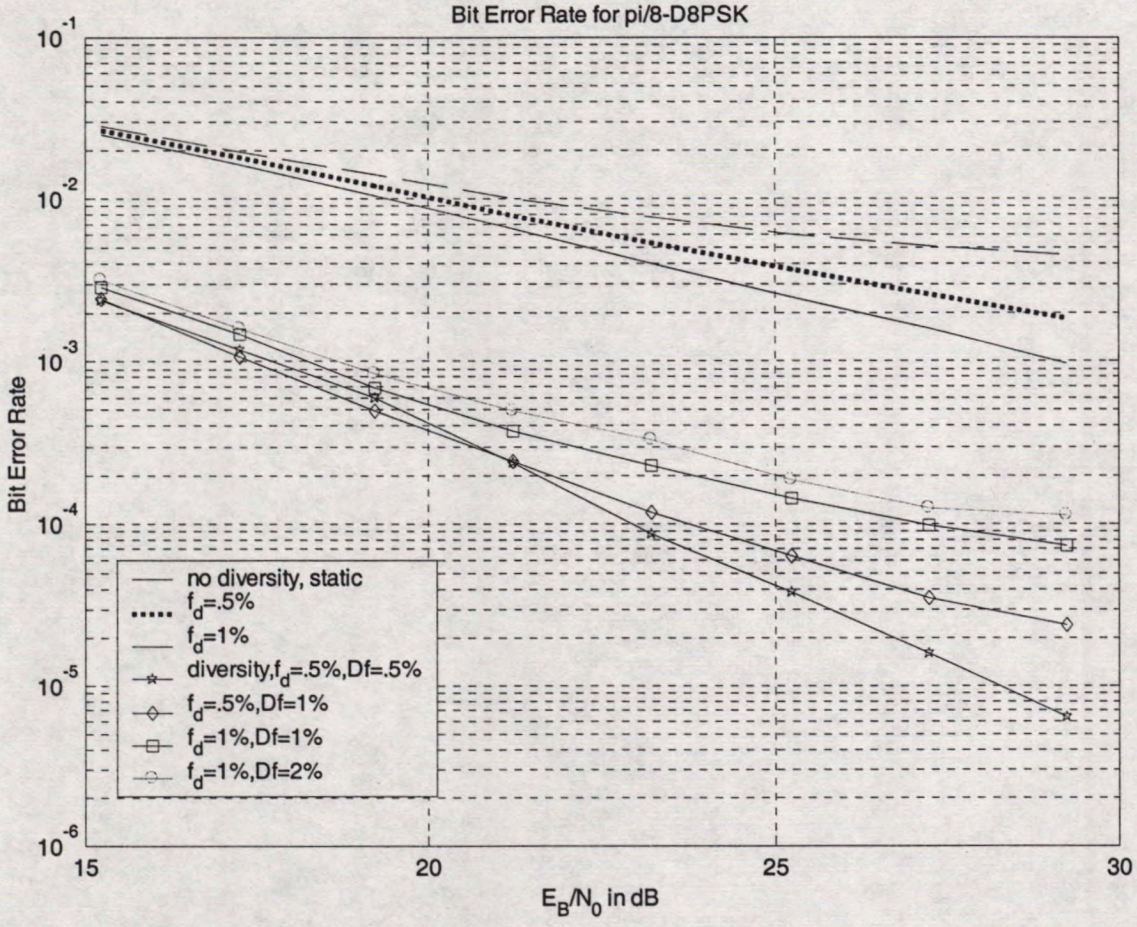

Figure 8 Bit Error rate for π/8 D8PSK. The maximum Doppler (f_d) is indicated in the legend as a percentage of the sub-carrier spacing. The up-link carrier frequency errors are uniformly distributed over a range of $-\Delta f$ to $+\Delta f$ as shown in the legend. The sampling clock errors are uniformly distributed in a range –10 to +10 PPM.

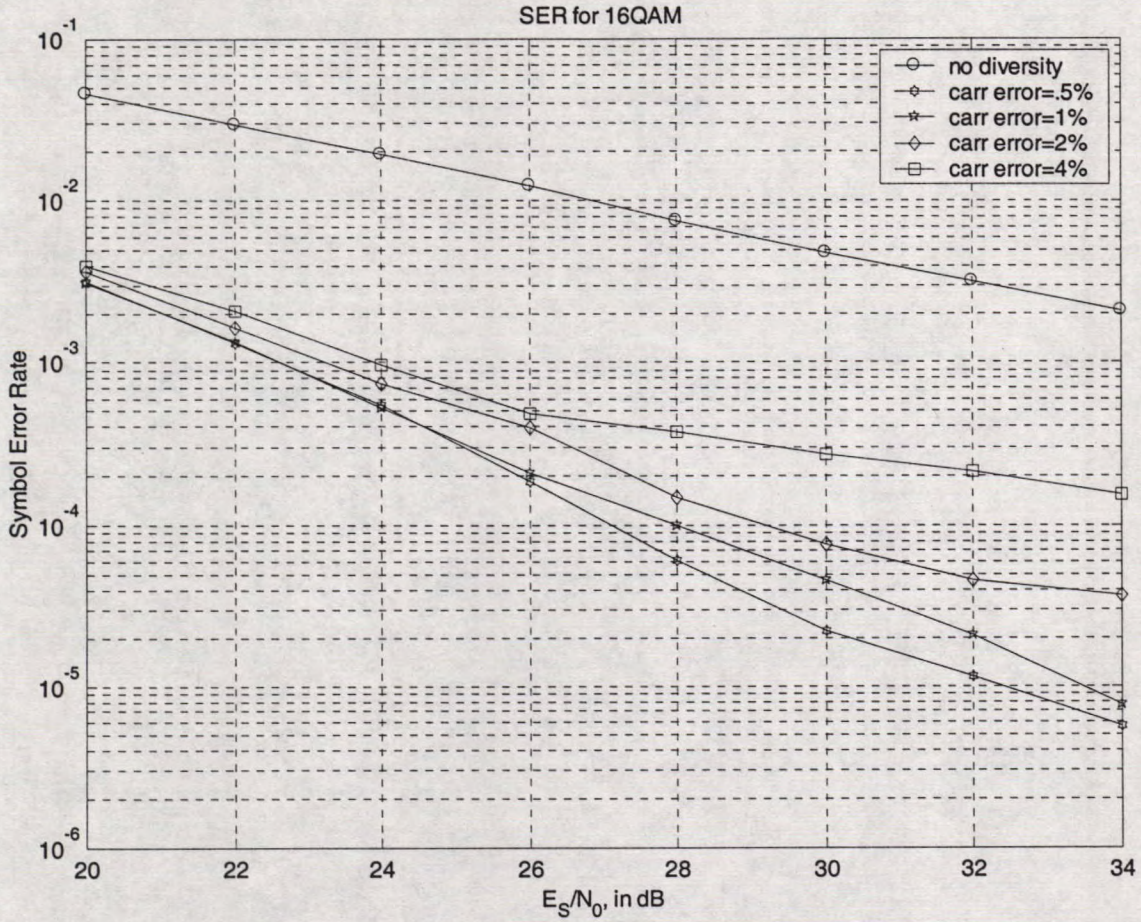

Figure 9 Symbol Error rate for 16QAM. The maximum Doppler (f_d) is the same for all curves, and equals 1% of the sub-carrier spacing. The up-link carrier frequency errors are uniformly distributed over a range of $-\Delta f$ to $+\Delta f$ as shown in the legend. The sampling clock errors are uniformly distributed in a range –10 to +10 PPM.

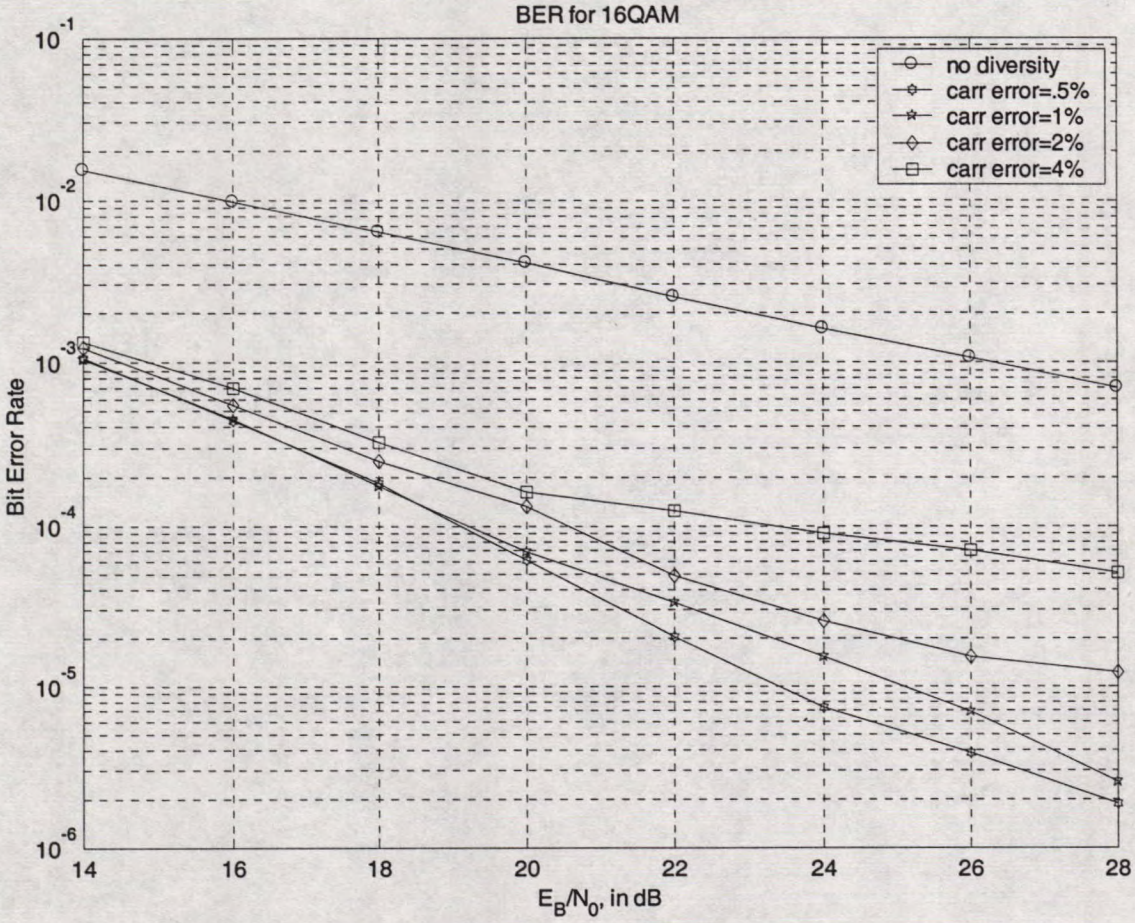

Figure 10 Bit Error rate for 16QAM. The maximum Doppler (f_d) is the same for all curves, and equals 1% of the sub-carrier spacing. The up-link carrier frequency errors are uniformly distributed over a range of $-\Delta f$ to $+\Delta f$ as shown in the legend. The sampling clock errors are uniformly distributed in a range –10 to +10 PPM.

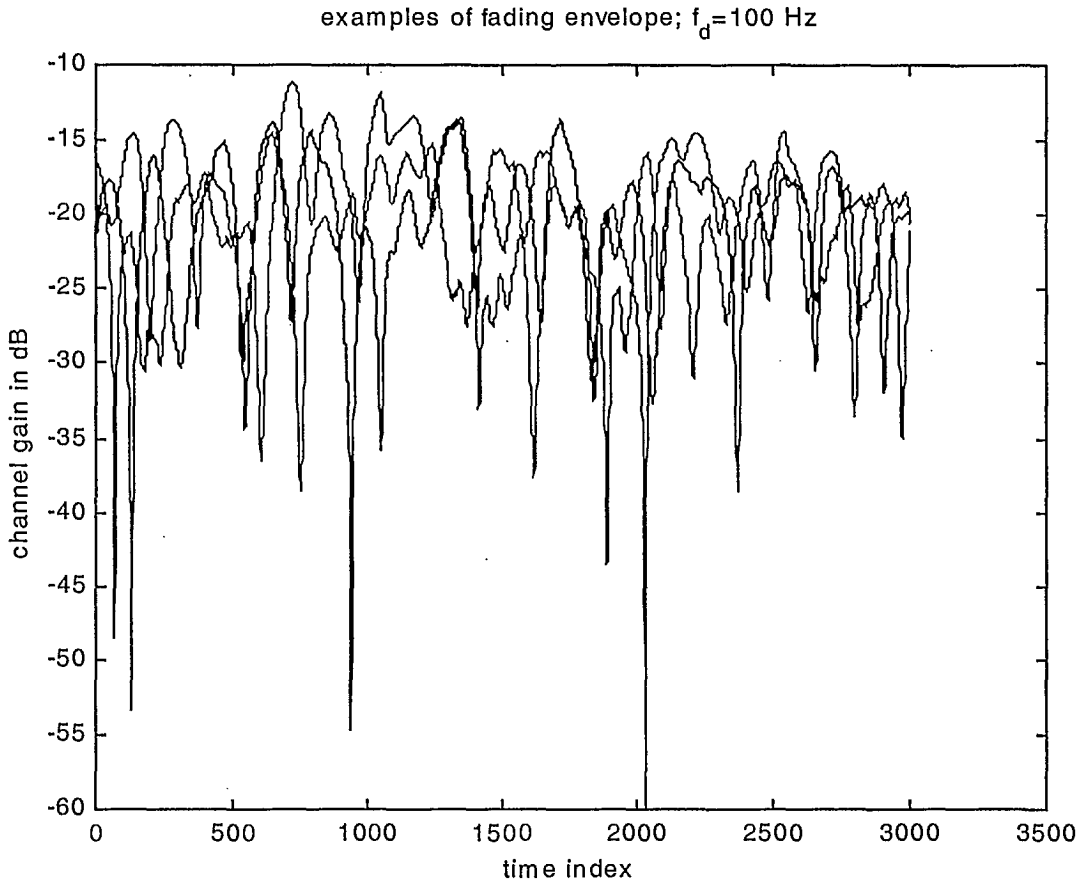

Figure 11 Envelopes of the fading channels presented to three uplink sub-carriers. These results are based on a Doppler shift of 100 Hz. Notice that the three sub-channels experience deep fades at different time instants. The fade depth on each of the 3 sub-channels exceeds 30 dB on two of the sub-channels.

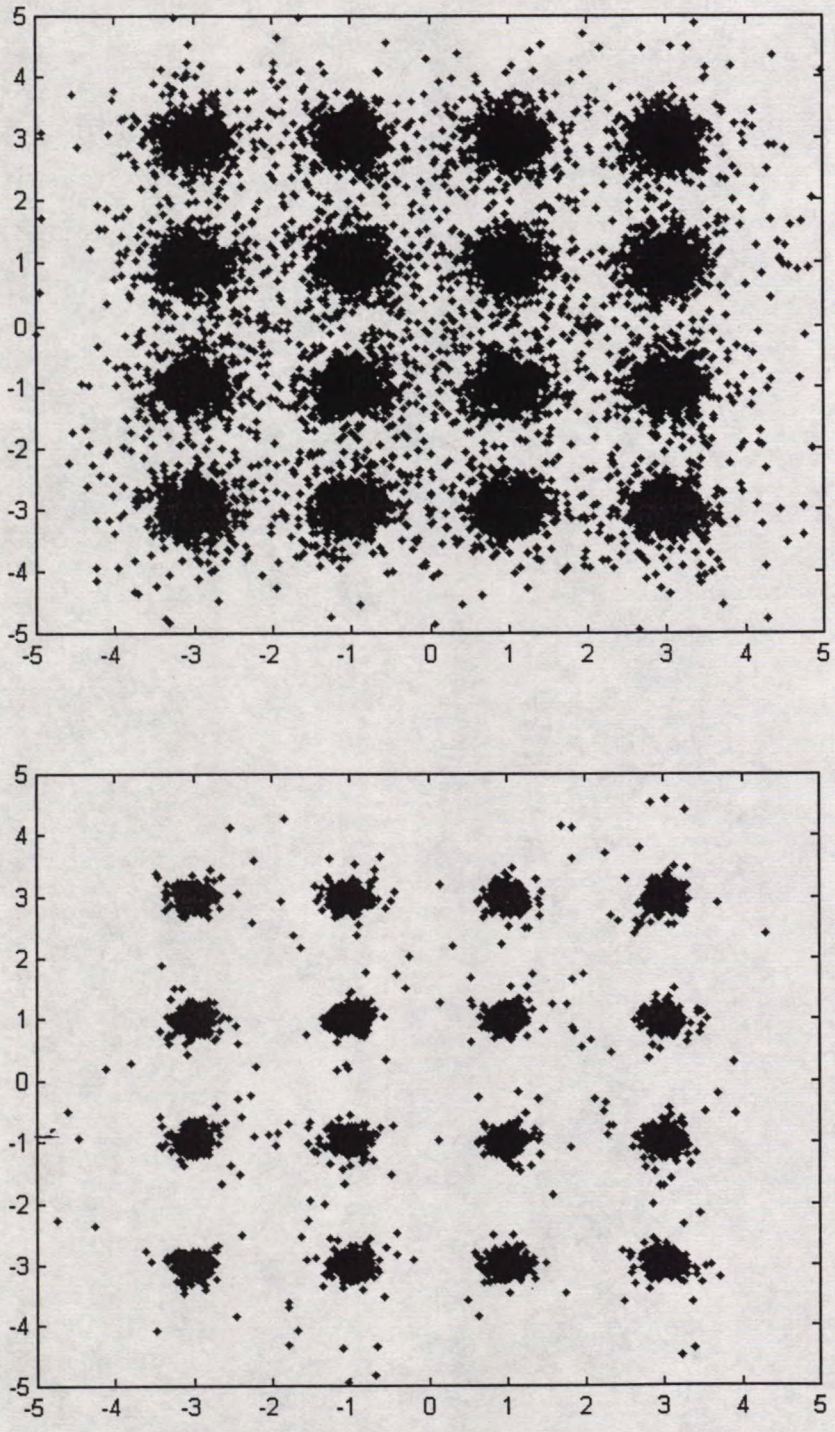

Figure 12Constellation diagrams for 16QAM demodulator under fading. Top: no diversity. Bottom: second order diversity. In both cases, the Doppler spread = 100 Hz.

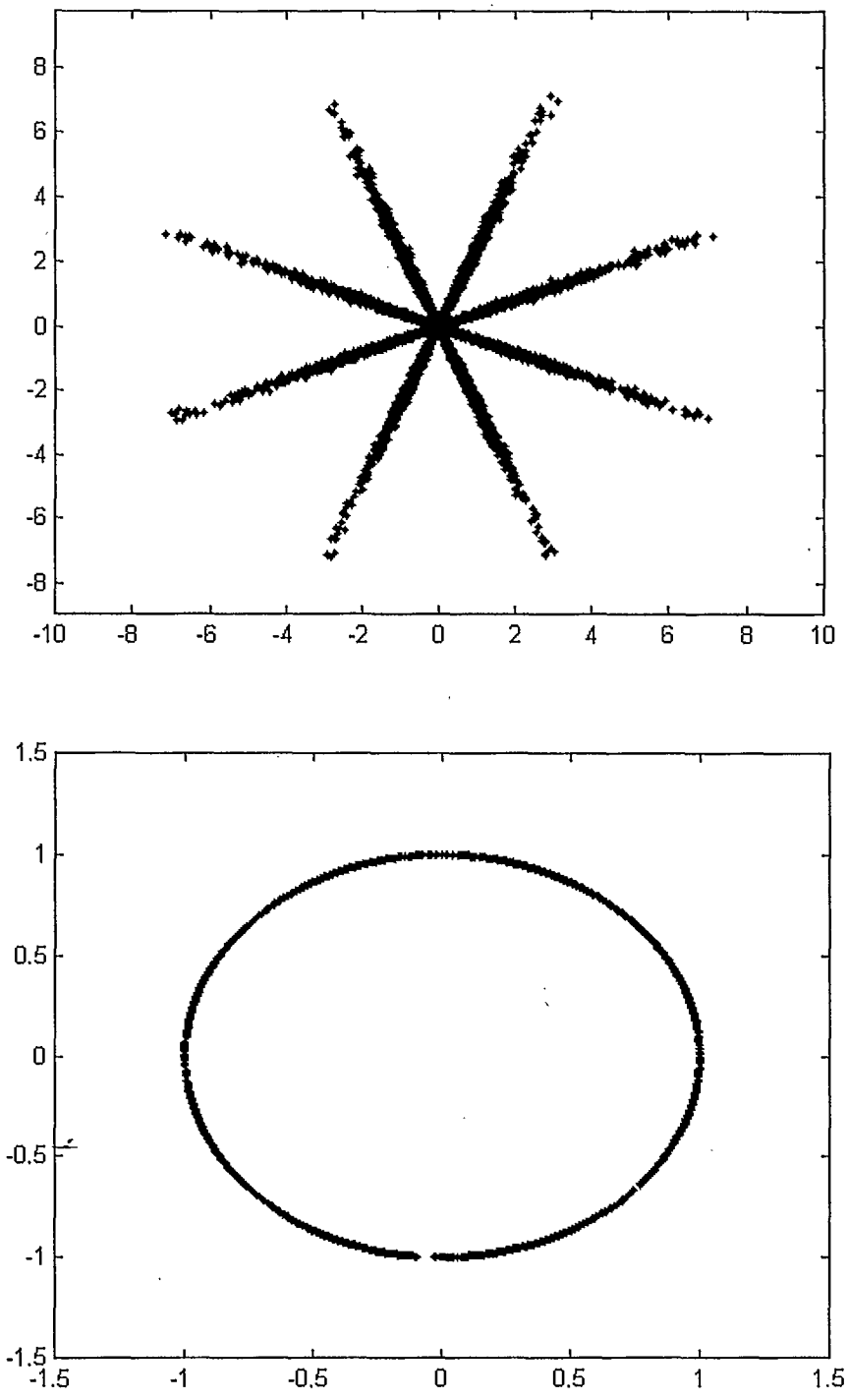

Figure 13Constellation diagram in an D8PSK demodulator with no diversity. The Doppler spread = 100 Hz. Top: at the output of the differential data detector. Bottom: ignores the magnitude variations at the output of the data detector.

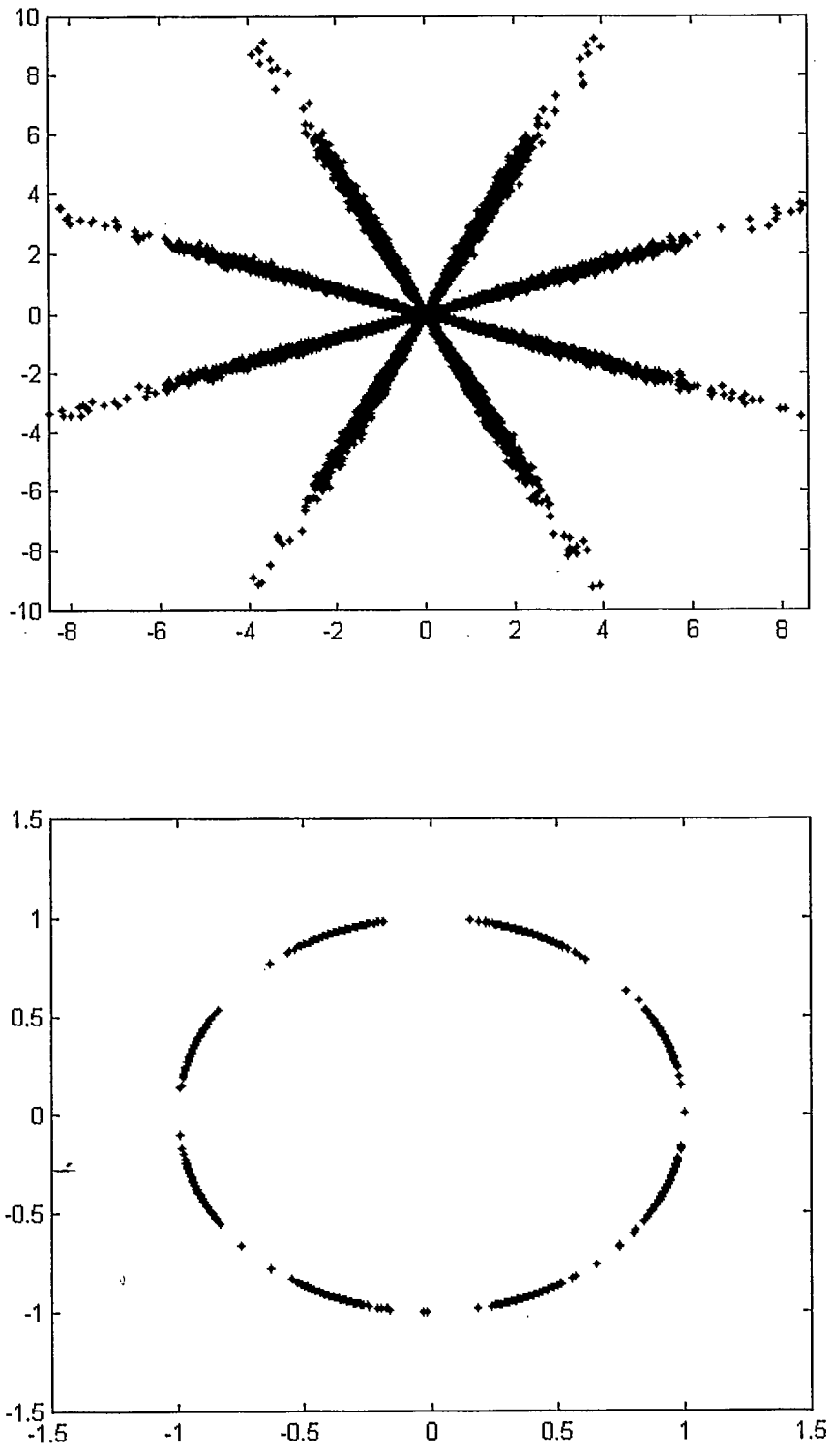

Figure 14Constellation diagrams in an D8PSK demodulator that employs second-order diversity. Top: at the output of the equal-gain combiner. Bottom: ignores the magnitude variations of the equal gain combiner.

References

[1] El-Tanany, M.S.; Yiyan Wu; Hazy, L., " OFDM uplink for interactive broadband wireless: analysis and simulation in the presence of carrier, clock and timing errors", *IEEE Transactions on Broadcasting*, Vol.47, no.1; March 2001, Page(s): 3 –19

[2] Yoshihiko Akaiwa "Introduction to Digital Mobile Communications", Wiley Series in Telecommunications, Wiley Interscience, 1997

[3] S. Sampei and T. Sunaga, "Rayleigh fading compensation method for 16QAM in digital land mobile radio channels", VTC89, p. 640-646

[4] L.E. Miller, J.S. Lee "BER expressions for differentially detected $\pi/4$-DQPSK modulation", IEEE Trans. Comm., vol 46, pp. 71-81, Jan 1998

[5]R.E. Ziemer, R.L. Peterson, "Introduction to digital Communication", second edition, Prentice Hall, 2001

DATE DUE

10. MAR 03			